NANO LETTERS

Letter

pubs.acs.org/NanoLett

Quantifying Surface Roughness Effects on Phonon Transport in Silicon Nanowires

Jongwoo Lim,[†,∥,#] Kedar Hippalgaonkar,[§,∥,#] Sean C. Andrews,[†,‡,∥] Arun Majumdar,[§,∥,⊥] and Peidong Yang*[,†,‡,∥]

[†]Department of Chemistry, [‡]Department of Materials Science and Engineering, and [§]Department of Mechanical Engineering, University of California, Berkeley, California 94720, United States

[∥]Materials Sciences Division, Lawrence Berkeley National Laboratory, Berkeley, California 94720, United States

Supporting Information

ABSTRACT: Although it has been qualitatively demonstrated that surface roughness can reduce the thermal conductivity of crystalline Si nanowires (SiNWs), the underlying reasons remain unknown and warrant quantitative studies and analysis. In this work, vapor−liquid−solid (VLS) grown SiNWs were controllably roughened and then thoroughly characterized with transmission electron microscopy to obtain detailed surface profiles. Once the roughness information (root-mean-square, σ, correlation length, L, and power spectra) was extracted from the surface profile of a specific SiNW, the thermal conductivity of the same SiNW was measured. The thermal conductivity correlated well with the power spectra of surface roughness, which varies as a power law in the 1−100 nm length scale range. These results suggest a new realm of phonon scattering from rough interfaces, which restricts phonon transport below the Casimir limit. Insights gained from this study can help develop a more concrete theoretical understanding of phonon−surface roughness interactions as well as aid the design of next generation thermoelectric devices.

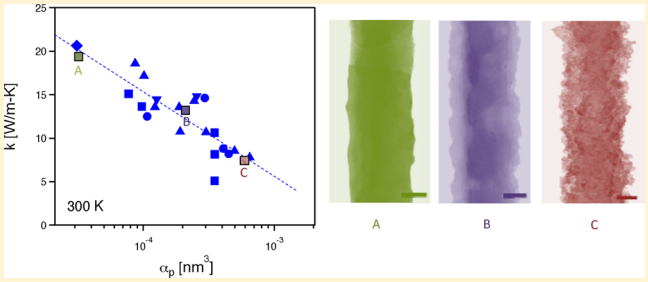

KEYWORDS: *Nanowire, silicon, roughness, thermoelectrics, thermal conductivity, phonons*

Recent studies have employed various methods to suppress phonon propagation as a strategy toward realizing efficient and cost-effective thermoelectric devices.[1−6] Chiritescu and Cahill et al. demonstrated that disordered layers of WSe_2 exhibited dramatically low thermal conductivity due to interface phonon scattering from random stacks of adjacent layers,[4] while Kim et al. were able to reach a thermal conductivity below the 'alloy limit' by embedding ErAs nanoparticles in crystalline $In_{0.53}Ga_{0.47}As$ to efficiently scatter a broad range of phonons at the heterogeneous interfaces.[5] While those studies used relatively exotic materials, Joshi et al. showed that even nanostructured bulk (nano-bulk) Si/Ge alloys exhibit reduced thermal conductivity via increased phonon scattering at grain boundaries.[6]

Similar to nano-bulk Si/Ge alloys, single-crystalline Si nanowires (SiNWs) have also shown depressed thermal conductivity due to phonon scattering from the nanowire surface. However, unlike previously mentioned systems, all of the factors that can influence phonon propagation have not been quantitatively studied. It has previously been reported by Li et al. that when the diameter of smooth single-crystal SiNWs that are grown by the vapor−liquid−solid (VLS) process reduces below 150 nm, the thermal conductivity is significantly lower than the bulk value and can closely follow predictions based on Boltzmann transport theory, assuming diffuse boundary scattering as the dominant phonon scattering mechanism.[7] Specifically, the thermal conductivity at 300 K ranges from 40 to 9 W/(m K) for SiNWs with diameters from 115 to 22 nm, respectively. To help explain this dependence, Mingo et al. proposed that despite the smooth surface nature of VLS SiNWs, phonon-surface boundary scattering is diffusive rather than specular.[8] This diameter-limited thermal conductivity based on diffuse phonon scattering at surfaces follows what has been described as the Casimir limit. Although the smooth VLS SiNWs show thermal conductivity reduction, roughened SiNWs produced by electroless etching of Si wafers (EE-SiNWs) were found to produce even lower thermal conductivity, as low as 1.6 W/(m K) for a SiNW of 56 nm diameter at 300 K.[1] This surprising result of thermal conductivity below the Casimir limit cannot be explained and warrants more quantitative study.

While the exact mechanism of phonon-roughness scattering is not clearly understood, there have been various attempts at developing theories behind such interactions.[9−16] One such study by Martin et al. employed the Born approximation toward phonon scattering to explain the large suppression in thermal conductivity.[9] They proposed that the roughness

Received: February 12, 2012
Revised: April 1, 2012
Published: April 23, 2012

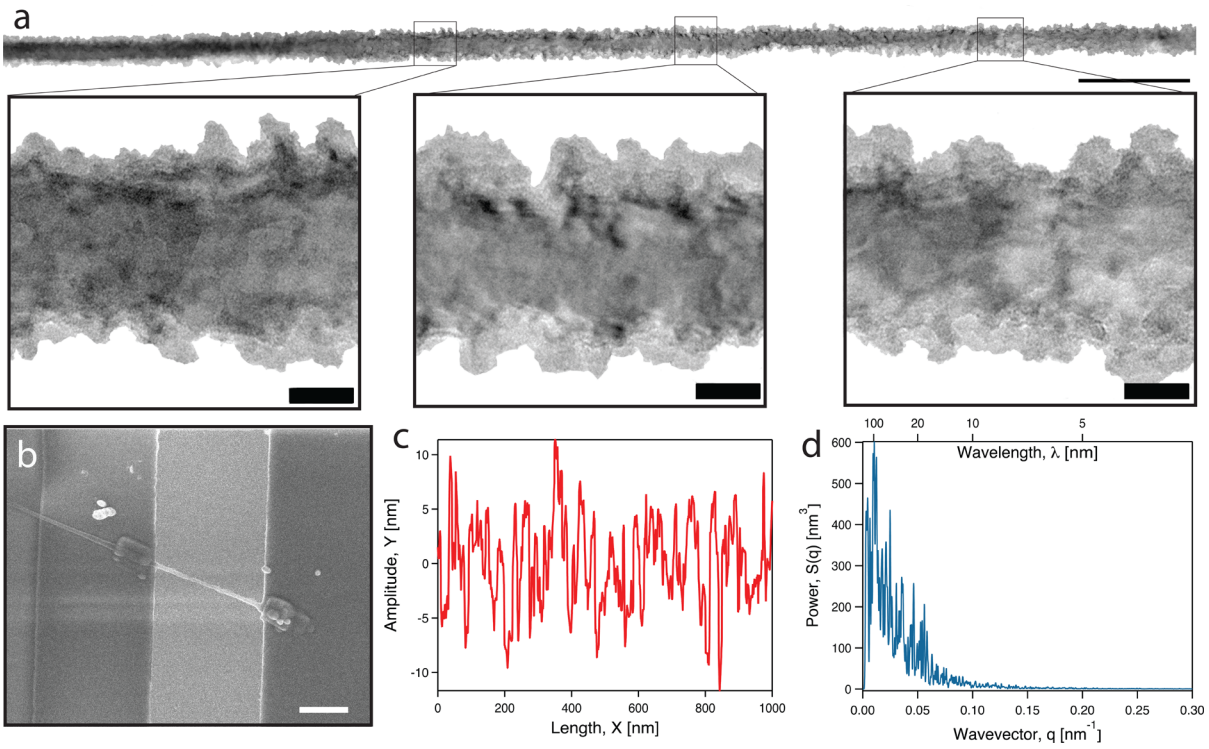

Figure 1. Surface roughness characterization. (a) Serial TEM images of a SiNW along the length with zoomed-in images at different positions. (b) SEM image of the identical nanowires from (a) on thermal measurement device. (c) Surface profile from serial TEM images. Full length is sectioned by 1 μm followed by fifth-order background elimination. (d) Averaged power spectrum from sectioned surface profiles. Scale bars for panel a are 500 and 20 nm, and panel b is 1 μm.

causes an alteration in the phonon dispersion and used perturbation theory to explain the enhanced scattering. Carrete and Mingo et al, however, believe the Born approximation is invalid at phonon wavelengths similar to the size of the scatterer.[10] Instead, they used an atomic level investigation for 2.2 nm diameter SiNWs with surface disorder to conclude that reducing the thermal conductivity by 1 order of magnitude is difficult. Using another approach, Moore et al. proposed a backscattering mechanism by using Monte Carlo (MC) simulations of SiNWs with sawtooth structures but could still not fully explain the large decrease in thermal conductivity.[11] More recent indirect MC simulations by Wang et al. proposed multiple scattering of phonons at the rough surface, while also accounting for impurity scattering, in order to fit their simulation to the experimental data of Hochbaum et al.[12] However, the random nature of roughness on the EE-SiNWs was not taken into account, which presumably could lead to frequency-dependent scattering from the surface. While these theoretical works shed some light on the dependence of thermal conductivity on rough surfaces, experimental determination of the dependence of thermal conductivity on surface roughness of SiNWs is still lacking.[18,19]

This work introduces a quantitative correlation between thermal conductivity and surface roughness by considering the full length of SiNWs under measurement. As opposed to EE-SiNWs, which are prepared from doped wafers, intrinsic VLS-grown SiNWs were etched in a controlled manner to create roughened surfaces. With this approach, the possible effects of impurity phonon scattering are eliminated.[1,7,8] We characterize the roughness on the roughened SiNWs by transmission electron microscopy (TEM) and statistically extract parameters to quantify the roughness on the surface. We found that root-mean-square (σ) and correlation length (L) of surface roughness do not individually correlate that well with the thermal conductivity. We introduce in this work a coefficient obtained from power law behavior of the roughness power spectrum at higher frequencies (α_p), which seems to correlate well with thermal conductivity reduction in single crystalline SiNWs.

Experimental Section. SiNWs having smooth surfaces were grown via the VLS growth mechanism using Au nanoparticles. Briefly, monodispersed Au nanoparticles were used as catalysts on a Si(111) wafer. The wafer was heated to 850 °C, while a mixture of $SiCl_4$ and H_2/Ar (1:9) was flown into the system. This synthesis process produced single-crystal Si nanowires with smooth surfaces grown along the ⟨111⟩ direction. More details about SiNW growth and conditions can be found elsewhere.[20,21] After growth, the Si die was immersed in buffered hydrofluoric acid (BHF, ammonium fluoride:hydrofluoric acid = 5:1), rinsed in deionized (DI) water, and then immersed in KI/I_2 solution to remove the Au residue. To induce roughness, two different processes were employed, each showing distinctly unique roughness features (Supporting Information Figure 1), which enabled us to study a variety of rough surfaces of SiNWs.

Surface Roughening Process 1. Prior to the surface roughening steps, the native oxide on the SiNWs was etched in HF vapor, and the collection of SiNWs was sonicated with DI water. When added to a mixture of $AgNO_3$ (1.74×10^{-3} M) and HF (3.53 M), the following reactions took place: The SiNW surface becomes oxidized as a result of a galvanic displacement reaction between Ag^+ ions and Si, which is then subsequently etched by HF. Metallic Ag nanoclusters grow on

dx.doi.org/10.1021/nl3005868 | Nano Lett. 2012, 12, 2475−2482

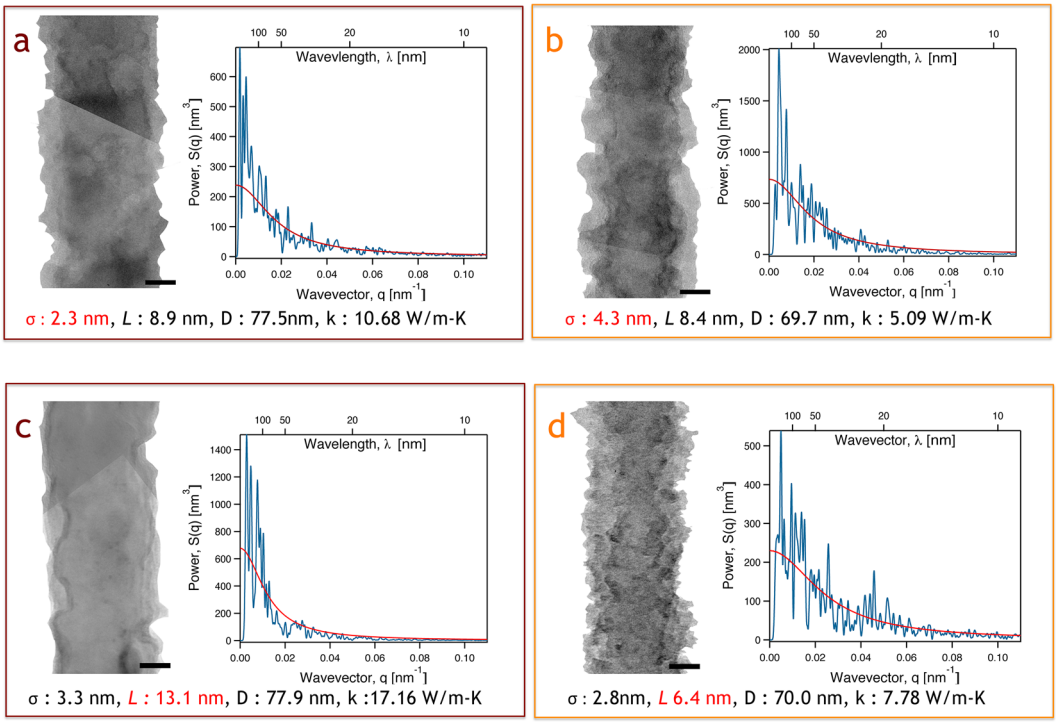

Figure 2. Extraction of σ and L from TEM images and their effect on thermal conductivity. (a,b) rms (σ) effect on thermal conductivity and (c,d) correlation length (L) effect on thermal conductivity. All scale bars are 1 μm.

the surface where the initial reduction of Ag^+ ions took place, thereby indicating where Si was etched.[22−24]

$$4Ag^+_{(aq)} + Si_{(s)} + 6F^-_{(aq)} \rightarrow 4Ag_{(s)} + SiF_6^{2-}{}_{(aq)} \quad (1)$$

After 2 min, the reaction was quenched with excessive amounts of DI water, and then the solution was centrifuged to separate the SiNWs. Once isolated, they were immersed in concentric nitric acid for 30 min to remove residual Ag nanoclusters. Suspended SiNWs were retrieved after repeating the centrifuge and rinsing process (Supporting Information Figure 1).

Surface Roughening Process 2. SiNWs were immersed in a mixture of $AgNO_3$ (1.74×10^{-3} M), HF (3.53 M) and H_2O_2 (5.57 M) solution for 3 min.[22] The reaction was followed with a DI water rinse and immersion into concentric nitric acid for residual Ag nanoparticle removal. Since the Ag nanoparticles are abundant and etching occurs only locally around them, the surface of SiNWs in both etching conditions showed a random, rough morphology (Supporting Information Figure 1). After treatment, roughened SiNWs were transferred to a TEM grid for surface analysis and physical manipulation.

The surface roughness of SiNWs was characterized by TEM. A series of images at 80 000× magnification were taken along the length of each SiNW and then stitched together, which enabled us to obtain information about the surface roughness along the entire length (Figure 1a). The diameter is obtained from the TEM images and defined by assuming a circular cross section at each point along the SiNW. Therefore, the average diameter of the entire SiNW is obtained from the average of all the individual cross sections. After TEM characterization, those specific individual SiNWs were manipulated onto prefabricated microdevices to measure the thermal transport properties (Figure 1b).[25] To reduce the thermal contact resistance, a Pt/C composite was deposited on both ends of the nanowire using electron beam induced deposition (EBID) inside a FEI-Strauss Dual Beam FIB (Supporting Information Figure 2). This method was used previously in literature and was successful in reducing thermal contact resistance for different materials.[26,27] Since only a 2−6 μm long section of the wire bridges the thermal device, only the roughness of that specific active segment between the contacts was considered in all calculations. Additionally, since curvature of even a 2−6 μm segment can affect the roughness measurement, surface profiles were sequentially analyzed along the length in 1 μm segments at a time (Figure 1c). To remove any marginal curvature effects, a fifth-order polynomial was used to subtract any background curvature. This procedure was insensitive to the order of polynomial chosen, as any polynomial higher than 5 produced the same quantitative result. After background subtraction, the rms and the power spectrum of each 1 μm section were averaged to generate the entire nanowire's rms, σ, and power spectrum, $S(q)$, respectively (Figure 1d).

Martin et al. postulated based on the Born approximation[9] that the frequency-dependent boundary scattering rate $\tau_{i,j}^{-1}(E)$ can be represented by a surface integral in energy, $S(E')$, where the integral is taken over the area of the surface of constant energy, E', as

$$\tau_{i,j}^{-1}(E) \propto \int_{E'=E_i} \frac{S(q)}{\nabla_{\mathbf{k}'} E'(\mathbf{k}')} dS_i(E'),\ q = \mathbf{k}' - \mathbf{k} \quad (2)$$

Here they considered a phonon with wavevector $\mathbf{k}$ from branch i scattering to a phonon with wavevector $\mathbf{k}'$ from branch j. Also, $S(q)$ is the Fourier transform of the spatial autocorrelation function or, in other words, the power spectrum, the dilated rough surface that scatters the phonons, which constitutes the perturbed Hamiltonian H' allowing for the transition from the incoming wavevector, $\mathbf{k}$ to the scattered wavevector $\mathbf{k}'$. Sadhu and Sinha, using a wave-like phonon

dx.doi.org/10.1021/nl3005868 | Nano Lett. 2012, 12, 2475−2482

transport approach, considered coherent scattering of phonons from a rough surface and presented that for modes at frequency ω:[17]

$$l_{mn}^{-1}(\omega) \propto \sum_{pq} S(q),\ q = k_{mn} - k_{pq} \tag{3}$$

where $l_{mn}^{-1}(\omega)$ is the mean attenuation length for those phonons scattering from incident direction k_{mn} to a scattered direction k_{pq} and $S(q)$ is the power spectrum. Thus, in order to understand scattering of phonons from a rough surface, experimental determination of $S(q)$ is crucial.

It is common to assume that the autocovariance function of a random rough surface follows an exponential curve given by $C_E(r)$ as also evidenced in literature shown in eq 4 below:[9,28−31]

$$C_E(r) = \sigma^2 e^{-r/L} \tag{4}$$

where $C_E(r)$ is the autocovariance function of the Si surface roughness, σ is the rms value of the extracted surface profile and L is the correlation length, which is a statistical parameter that determines the decay of the autocovariance and is related to the lateral length scale of the roughness. By convolution theorem, the power spectrum is the Fourier transform of the autocovariance function, yielding a Lorentzian form given by

$$S_E(q) = 2L\Delta^2 \frac{1}{[1 + (2\pi Lq)^2]} \tag{5}$$

In this study, one-dimensional (1-D) power spectrum derived from the fast Fourier transform (FFT) was calculated for the surface profile with ordinary wavevectors given by q in units of nm^{-1}. As a first approximation, since previous theoretical work has assumed an exponential autocovariance fit for calculating surface roughness, the Lorentzian defined in eq 5 is used to extract L from the total power spectrum, $S(q)$.[9,28,29]

As seen in Figure 2, this method produced σ and L values from TEM images of individual rough SiNWs. Two SiNWs with comparable L (8.9 and 8.4 nm) and similar D (77.5 and 69.7 nm) are shown in Figure 2a,b, respectively. The TEM images clearly depict the significantly different rms values of the two SiNWs (σ = 2.3 and 4.3 nm), which lead to their correspondingly different thermal conductivities (10.68 and 5.09 W/(m K), respectively). In Figure 2c,d, on the other hand, the nanowires have comparable diameters D (78 and 70 nm) and σ values (∼ 3.3 and ∼2.8 nm), respectively. However, the SiNW in Figure 2d has roughness with L ∼ 6.4 nm, which is half the value of that for the SiNW in Figure 2c (L ∼ 13.1 nm). A smaller value of L corresponds to roughness features occurring at a shorter length scale, which scatter broadband phonons more effectively.[9,15,28,29] The resulting thermal conductivity at 300 K of the SiNW in Figure 2d [7.78 W/(m K)] is lower than that of the nanowire in Figure 2c [17.16 W/(m K)]. This provides evidence toward enhanced phonon-surface scattering in SiNWs with shorter L.

The thermal conductivities of these and other SiNWs are plotted as a function of temperature in Figure 3. Nanowires with comparable L (8.4 − 8.9 nm) and D (67.9 − 79.8 nm) were selected in Figure 3a, while nanowires with comparable rms (σ = 2.8 − 3.3 nm) and D (70 − 77.9 nm) were chosen in Figure 3b. Clearly, the increase in rms from σ ∼ 0 (as-grown) to 4.3 nm drops the thermal conductivity from 25 to 5.09 W/(m K) at 300 K. Similarly in Figure 3b, as σ remained

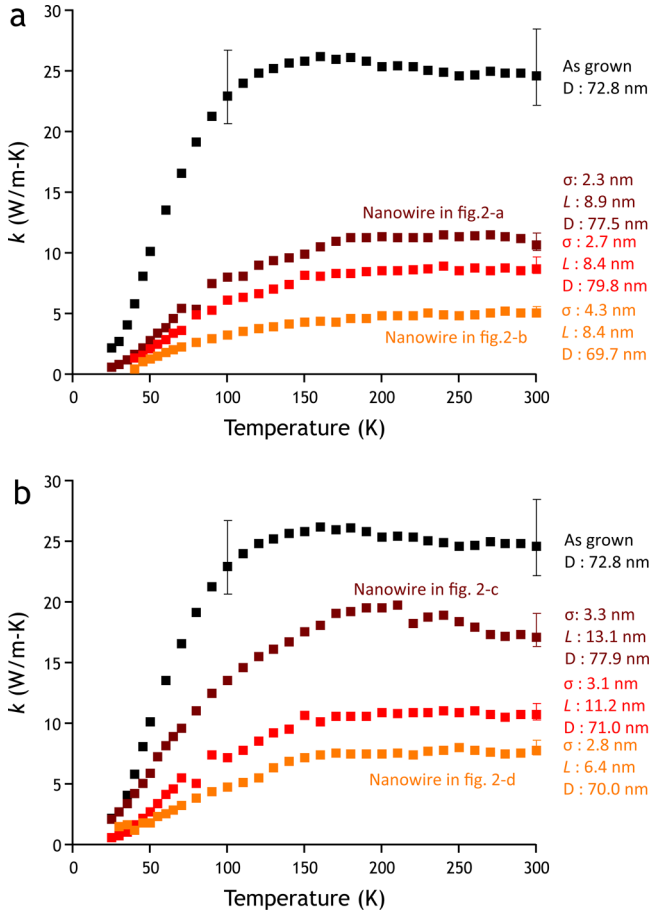

Figure 3. Thermal conductivity with temperature as a function of L and σ. (a) Thermal conductivity dependence on σ with controlled L and D. (b) Thermal conductivity dependence on correlation length L with controlled σ and D.

comparable and L decreased (down to 6.4 nm), a drop in thermal conductivity from 24.63 to 7.78 W/(m K) was observed. Thus, utilizing the full power spectrum of the roughness profile and looking at the σ and L values, we can predict that rougher wires with higher σ and lower L tend to have a lower thermal conductivity.

However, in order to understand the nature of scattering from the surface of the nanowires, we need to consider phonon wavelengths as well, which previous studies have lacked. In using the kinetic theory for phonons, we can consider that at any temperature, the order of magnitude estimate for a dominant wavelength carrying the heat is given by $\lambda_{dom} \sim (2h\nu_g)/(k_B T)$, where ν_g is the average group velocity of the phonons at thermodynamic temperature T.[32,33] At 300 K, λ_{dom} is ∼1 nm. However, in reality, there is a large spectrum of phonon wavelengths that contribute to the thermal conductivity. As shown in Figure 4a (reproduced with permission from A. Henry et al. and publishers *J. Comput. Theor. Nanosci.*),[34] a strong spectral dependence of the contribution of phonons to thermal conductivity exists, and up to 80% of the thermal conductivity at 300 K in bulk Si can arise from phonon wavelengths ranging from 1 to 100 nm. Using this as a starting point for analysis and taking a careful look at this wavelength bandwidth of the roughness power spectrum, $S(q)$, it is found that a power law fit captures the power spectrum more accurately (with a least-squares fit of >0.9 for all nanowires

dx.doi.org/10.1021/nl3005868 | *Nano Lett.* 2012, 12, 2475−2482

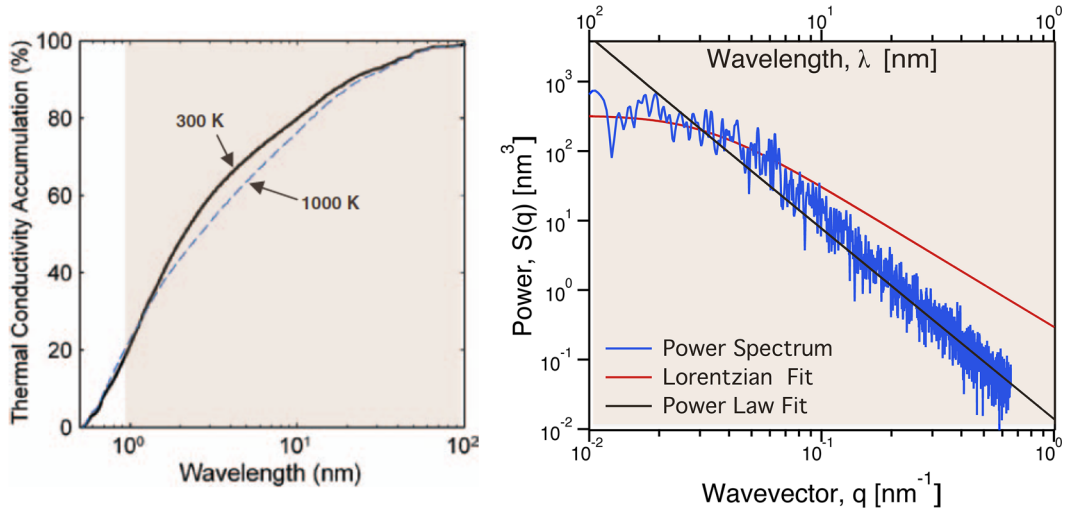

Figure 4. (a) Thermal conductivity accumulation as a function of wavelength at 300 and 1000 K (reproduced with permission from the authors and publishers in *J. Comput. Theor. Nanosci.*).[34] Roughly 80% of contribution to thermal conductivity at room temperature comes from phonons with wavelengths between 1 and 100 nm. (b) Roughness power spectrum at the selected length scales (1−100 nm). While the actual power spectrum is shown in blue, the Lorentzian fit used to extract σ and L is shown in red to be a poor fit at the relevant length scales. The power law fit shown in black captures the roughness better.

measured) than a Lorentzian, as shown in Figure 4b.[35] The fit used to then define the roughness is given by

$$S(q)_{10^{-2}\rightarrow 10^{0}} = \alpha_p \left(\frac{q_0}{q}\right)^n \quad (6)$$

where only wavevectors, q of the roughness from 10^{-2} to 10^{0} nm^{-1} (1−100 nm) are considered; α_p and n are parameters derived from the fit; and q_0 = 1/0.313 nm is the inverse of the lattice constant of Si in the ⟨111⟩ direction. The exponent n is related to the nature of the roughness, which is roughly the same for all nanowires measured in this study, and was determined to be n_{rms} = 2.77 and $n_{standard\ deviation}$ = 0.075 (Supporting Information Table 1). This indicates that the intentional etching of the VLS nanowires described in the earlier section produces a certain type of roughness where the relative amplitudes at different wavelengths or the ratio of amplitudes at different wavelengths, represented by the exponent n, remain roughly the same. On the other hand, α_p is related to the broadband roughness amplitude parameter of the nanowire surface at these relevant wavelengths. We expect a larger α_p for a rougher nanowire. Thus, the thermal conductivity is anticipated to be lower when the value of α_p is higher, while the exact functional dependence is difficult to ascertain.

In order to better understand the individual roles played by rms, diameter, correlation length, and the high-frequency amplitude term, α_p, toward reducing phonon propagation, the room temperature thermal conductivity of SiNWs as a function of different parameters is plotted in Figure 5a−f. Comparing Figure 5a,b, it can clearly be seen that rms exhibits a more pronounced impact on the thermal conductivity than the diameter. This clearly indicates that for rough nanowires, rms, rather than diameter (within the range measured), is the major limiter of phonon propagation. Further, as illustrated in Figure 5c, there is no clear dependence of thermal conductivity purely on the correlation length L, which indicates that L by itself does not capture the surface roughness accurately. The fact that the rms rather than the diameter has more influence on phonon transport is qualitatively different from the trend observed with smooth SiNWs, where boundary scattering occurs in the diffusive regime.[7,8] In this diffusive picture, the nanowire surface absorbs all phonons impinging upon it and thermalizes it and then, behaving as a blackbody (to ensure elastic scattering), re-emits the phonons at a rate proportional to the local temperature of the surface. In this new subdiffusive regime, where the thermal conductivity, k is lower than the Casimir limit, we first propose a dimensionless roughness correlation factor to define the total roughness, σ/L, which is based upon the following physical intuition: the magnitude of the roughness is (1) proportional to σ and (2) inversely proportional to L at 300 K (Figure 5d). While it is clear that σ and L are the important parameters that define the roughness of the surface, they do not directly represent the roughness parameter that is relevant for phonon scattering. Therefore, it is not surprising that although there seems to be a better trend of thermal conductivity with σ/L as opposed to that with σ or L individually, the correlation is not very strong and shows scatter.

Looking back at Figure 4b in detail, the Lorentzian fit does not capture roughness spectrum at the relevant wavelengths (1−100 nm) very well. Also, the roughness length scales that are relevant for phonon scattering are better captured in the power spectrum, which is represented by two parameters α_p and n. Since n is a constant across all the etched wires, what captures the roughness structure over the relevant phonon scattering band is the parameter α_p. Figure 5e plots the thermal conductivity as a function of α_p for various wires at 300 K, and a much stronger trend is observed. This indicates that directly relating the lateral length scale of the roughness to the wavelength bandwidth of phonons contributing to thermal conductivity is key to understanding the physics of roughness boundary scattering. Figure 5f plots the thermal conductivity as a function of α_p for the same wires at 100 K, which is a marginally better fit.

The enhanced scattering of phonons from rough surfaces observed in this study qualitatively follows predictions from earlier theoretical work. Separately, both Alvarez et al. and Moore et al. predicted stronger backscattering of phonons at

dx.doi.org/10.1021/nl3005868 | *Nano Lett.* 2012, 12, 2475−2482

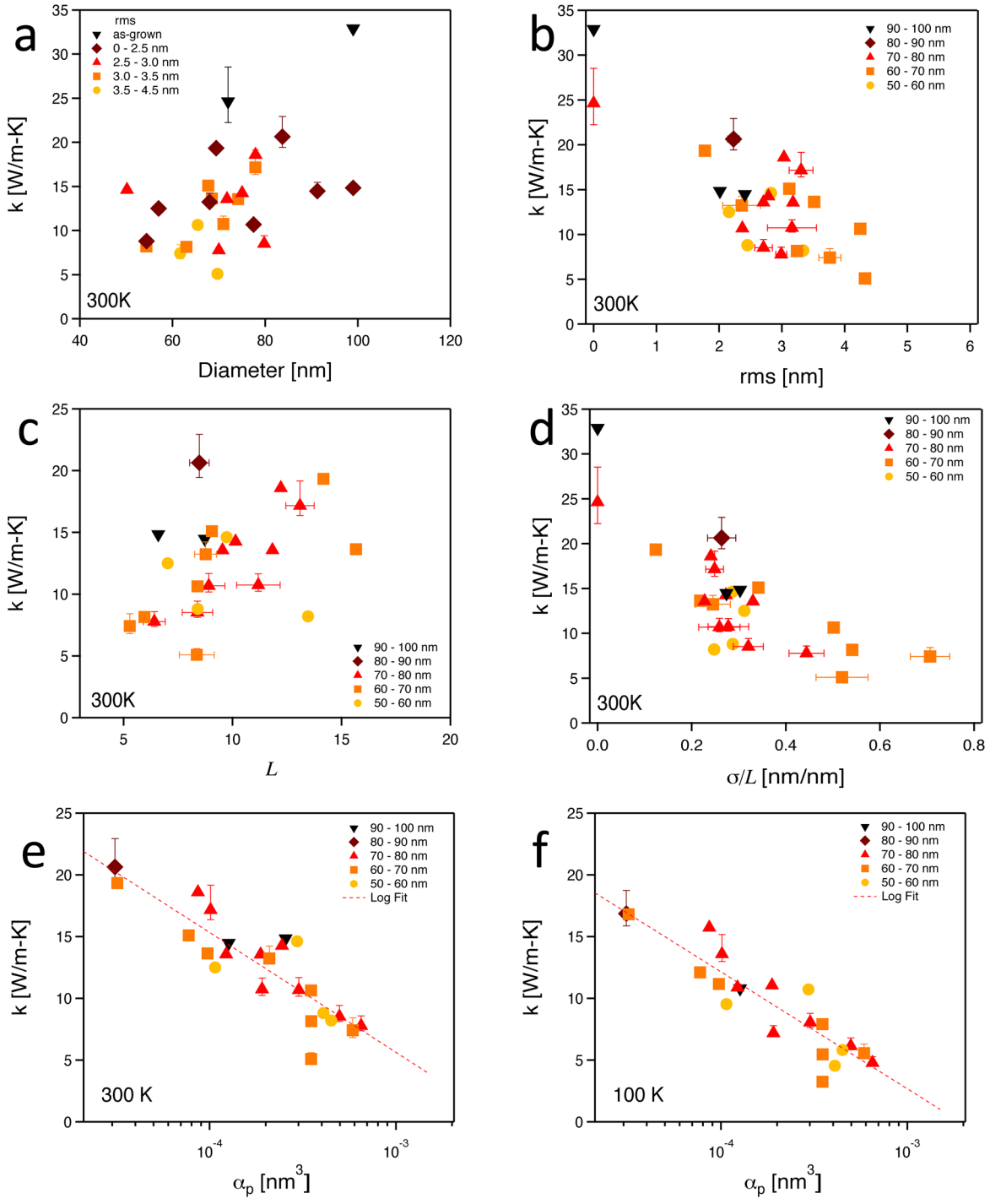

Figure 5. Thermal conductivity as a function of four roughness factors (σ, L, σ/L and α_p). (a). Thermal conductivity at 300 K as a function of diameter with different range of rms. (b). Thermal conductivity as a function of rms with different range of diameter. (c). Thermal conductivity as a function of L with different range of diameter. (d). Thermal conductivity as a function of σ/L for 300 K. Correlation between thermal conductivity and σ/L gets stronger than rms or D only and has a trend similar to Figure 3a in ref 9, except the discrepancy in L. (e,f) Thermal conductivity as a function of α_p (plotted on a log scale) at 300 and 100 K, respectively. As α_p increases, the wires are rougher, with wavelengths in the 1−100 nm range and the thermal conductivity drops significantly.

periodically rough surfaces with longer σ and shorter L by using phonon hydrodynamics and MC simulations, respectively.[11,13] However, direct application of this analysis is hindered by the nonuniform roughness profile obtained from the electrochemical etching technique, which may behave differently than the periodic structure. A possibly more applicable theory by Wang et al.[12] suggested that phonons are localized at the rough surface due to multiple boundary scattering occurrences within a single roughness feature on the surface. They pointed out that thermal conductivity decreases as features become sharper, which can be interpreted as a shorter L and higher σ. However, they did not look at the effect of high-frequency roughness that may selectively scatter phonons more effectively than the low-frequency ones.[12] Martin et al.[9] and Santamore et

dx.doi.org/10.1021/nl3005868 | Nano Lett. 2012, 12, 2475−2482

al.[31] use a perturbative approach due to the change in potential at the surface resulting in enhanced boundary scattering, however it remains to be seen if these claims are valid given the range of correlation lengths and rms we have observed in our work. While their study used a correlation length, L = 6 nm, our observed L varies from 5.3 to 15.7 nm, with rms values, σ, ranging from 1.8 to 4.3 nm. Sadhu et al. used a broader range of correlation lengths that fit the power spectrum and used a green Kubo analysis coupled with the Landauer formalism to extract attenuation lengths for all phonon modes. Some modes had reduced phonon group velocity in their analysis, which they postulated resulted in a lower thermal conductivity.[17]

However, none of these theoretical studies looked at the wavelength-dependent conductivity with scattering from the surface for a selective range of roughness wavelengths. To our best knowledge, our experimental work provides first evidence for frequency-dependent phonon scattering from rough surfaces. We hypothesize that as high-frequency roughness of the nanowire surface increases, there is enhanced boundary scattering, thus reducing the thermal conductivity significantly. This experimental study warrants further theoretical exploration of scattering of phonons from a rough boundary at specific relevant wavelengths in order to understand the exact correlation between the statistically defined α_p parameter and the thermal conductivity.

Every attempt was made at obtaining the most accurate and certain data possible, but there are, however, limitations to our method of characterizing roughness. First, TEM images are 2-D projections of a 3-D material. Therefore, roughness profiles from the projected surface images neglect hidden roughness features not occurring at the respective edge of the sample. But due to the isotropic nature of the etching process and the large number of samples measured, the determined relations found here are statistically meaningful. Second, the Lorentzian fitting curve to power spectrum is strongly sensitive to low-frequency peaks which account for not only rough surface but also the curvature of the SiNWs. Hence, the choice was made to fit a power law to the high-frequency section of the power spectrum only. Third, since L is calculated using the assumption that the autocovariance of the surface profile is an exponential, the uncertainty of L can be estimated based on the coefficient of determination from a least-squared fit, R^2, when eq 5 is used to fit the original power spectra. Hence, only the Lorentzian fitting functions where R^2 is larger than a certain value (0.63) are strictly chosen. Despite the relatively large uncertainty in L, as can be seen in Figure 5d, trends of the dependence of thermal conductivity, k with σ/L, are clearer than that of thermal conductivity purely with rms. In terms of the power law fit, the choice of frequency limits was informed from A. Henry et al.[34] First principle calculations, however, show a tighter phonon wavelength bandwidth contributing to thermal conductivity, and this bandwidth can also be significantly temperature dependent.[36,37] The thermal conductivity strongly correlates with the parameter, α_p, extracted from a power law fit of the roughness power spectrum, which opens up a new way of not only characterizing rough surfaces but also shedding some light on the possible physics at work.

In conclusion, this study has experimentally shown that surface roughness can be captured accurately by applying spectral techniques to the profile obtained from high-resolution TEM images. The study suggests that the surface roughness interacts with a broadband spectrum of phonons in SiNWs, resulting in decreased thermal conductivity due to frequency-dependent scattering. Additionally, the quantitative relationship between three independent roughness parameters, σ, L, and α_p, has been measured and shown to have a greater effect on the thermal conductivity of SiNWs than diameter. Specifically, the power spectra of the roughness with a power law fit in the wavelength range of 1−100 nm scale strongly with the reduction in thermal conductivity. With these results, it is clear that quantifying the surface roughness is crucial to both understanding the fundamental physics of phonon transport as well as engineering practical thermoelectric devices.

■ ASSOCIATED CONTENT

Ⓢ Supporting Information

Surface roughening process, HRTEM images of the surface, contact resistance measurement, and raw data. This material is available free of charge via the Internet at http://pubs.acs.org.

■ AUTHOR INFORMATION

Corresponding Author

*E-mail: p_yang@berkeley.edu.

Present Address

[⊥]U.S. Department of Energy, 1000 Independence Avenue SW, Washington, DC 20585

Author Contributions

[#]These authors contributed equally.

Notes

The authors declare no competing financial interest.

■ ACKNOWLEDGMENTS

We thank Sarah Brittman for image processing, Dr. Melissa Fardy for TEM imaging, and Dr. Erik Garnett, Dr. Hoon-E Jeong, Yunjeong Hwang, Dr. Hungta Wang, Dr. Jinyao Tang, Prof. Joel Moore and Prof. Chris Dames for discussion. This work was supported by the Director, Office of Science, Office of Basic Energy Sciences, Materials Sciences and Engineering Division, of the U.S. Department of Energy under contract no. DE-AC02-05CH11231.

■ REFERENCES

(1) Hochbaum, A. I.; Chen, R. K.; Delgado, R. D.; Liang, W. J.; Garnett, E. C.; Najarian, M.; Majumdar, A.; Yang, P. D. *Nature* **2008**, *451*, 163−U165.

(2) Boukai, A. I.; Bunimovich, Y.; Tahir-Kheli, J.; Yu, J.-K.; Goddard, W. A., III; Heath, J. R. *Nature* **2008**, *451*, 168−171.

(3) Tang, J.; Wang, H.-T.; Lee, D. H.; Fardy, M.; Huo, Z.; Russell, T. P.; Yang, P. *Nano Lett.* **2010**, *10*, 4279−4283.

(4) Chiritescu, C.; Cahill, D. G.; Nguyen, N.; Johnson, D.; Bodapati, A.; Keblinski, P.; Zschack, P. *Science* **2007**, *315*, 351−353.

(5) Kim, W.; Zide, J.; Gossard, A.; Klenov, D.; Stemmer, S.; Shakouri, A.; Majumdar, A. *Phys. Rev. Lett.* **2006**, *96*, 045901.

(6) Joshi, G.; Lee, H.; Lan, Y.; Wang, X.; Zhu, G.; Wang, D.; Gould, R. W.; Cuff, D. C.; Tang, M. Y.; Dresselhaus, M. S.; Chen, G.; Ren, Z. *Nano Lett.* **2008**, *8*, 4670−4674.

(7) Li, D.; Wu, Y.; Kim, P.; Shi, L.; Yang, P.; Majumdar, A. *Appl. Phys. Lett.* **2003**, *83*, 2934−2936.

(8) Mingo, N. *Phys. Rev. B* **2003**, *68*, 113308.

(9) Martin, P.; Aksamija, Z.; Pop, E.; Ravaioli, U. *Phys. Rev. Lett.* **2009**, *102*, 125503.

(10) Carrete, J; Gallego, L. J.; Varela, L. M.; Mingo, N. *Phys. Rev. B* **2011**, *84*, 075403.

(11) Moore, A. L.; Saha, S. K.; Prasher, R. S.; Shi, L. *Appl. Phys. Lett.* **2008**, *93*, 083112−083113.

(12) Wang, Z.; Ni, Z.; Zhao, R.; Chen, M.; Bi, K.; Chen, Y. *Phys. B (Amsterdam, Neth.)* **2011**, *406*, 2515−2520.

(13) Alvarez, F. X.; Jou, D.; Sellitto, A. *J. Heat Transfer* **2011**, *133*, 022402.
(14) Sellitto, A.; Alvarez, F. X.; Jou, D. *J. Appl. Phys.* **2010**, *107*, 114312.
(15) Liu, L.; Chen, X. *J. Appl. Phys.* **2010**, *107*, 033501.
(16) Chen, Y. R.; Jeng, M. S.; Chou, Y. W.; Yang, C. C. *Comput. Mater. Sci.* **2011**, *50*, 1932−1936.
(17) Sadhu, J.; Sinha, S. *Phys. Rev. B* **2011**, *84*, 115450.
(18) Hippalgaonkar, K.; Huang, B.; Chen, R.; Sawyer, K.; Ercius, P.; Majumdar, A. *Nano Lett.* **2010**, *10*, 4341−4348.
(19) Park, Y.-H.; Kim, J.; Kim, H.; Kim, I.; Lee, K.-Y.; Seo, D.; Choi, H.-J.; Kim, W. *Appl. Phys. A: Mater. Sci. Process.* **2011**, *104*, 7−14.
(20) Givargizov, E. I. *J. Cryst. Growth* **1975**, *31*, 20−30.
(21) Hochbaum, A. I.; Fan, R.; He, R. R.; Yang, P. D. *Nano Lett.* **2005**, *5*, 457−460.
(22) Huang, Z. P.; Geyer, N.; Werner, P.; de Boor, J.; Gosele, U. *Adv. Mater.* **2011**, *23*, 285−308.
(23) Peng, K. Q.; Yan, Y. J.; Gao, S. P.; Zhu, J. *Adv. Funct. Mater.* **2003**, *13*, 127−132.
(24) Peng, K. Q.; Wu, Y.; Fang, H.; Zhong, X. Y.; Xu, Y.; Zhu, J. *Angew Chem. In.t Ed.* **2005**, *44*, 2737−2742.
(25) Shi, L.; Li, D. Y.; Yu, C. H.; Jang, W. Y.; Kim, D. Y.; Yao, Z.; Kim, P.; Majumdar, A. *J. Heat Transfer* **2003**, *125*, 1209−1209.
(26) Yang, J.; Yang, Y.; Waltermire, S. W.; Gutu, T.; Zinn, A. A.; Xu, T. T.; Chen, Y.; Li, D. *Small* **2011**, *7*, 2334−2340.
(27) Mavrokefalos, A.; Pettes, M. T.; Zhou, F.; Shi, L. *Rev. Sci. Instrum.* **2007**, *78*, 34901.
(28) Goodnick, S. M.; Gann, R. G.; Sites, J. R.; Ferry, D. K.; Wilmsen, C. W.; Fathy, D.; Krivanek, O. L. *J. Vac. Sci. Technol., B: Microelectron. Nanometer Struct.−Process., Meas., Phenom.* **1983**, *1*, 803−808.
(29) Goodnick, S. M.; Ferry, D. K.; Wilmsen, C. W.; Liliental, Z.; Fathy, D.; Krivanek, O. L. *Phys. Rev. B* **1985**, *32*, 8171.
(30) Yamakawa, S.; Ueno, H.; Taniguchi, K.; Hamaguchi, C.; Miyatsuji, K.; Masaki, K.; Ravaioli, U. *J. Appl. Phys.* **1996**, *79*, 911−916.
(31) Santamore, D. H.; Cross, M. C. *Phys. Rev. B* **2001**, *63*, 184306.
(32) Ziman, J. M. *Electrons and phonons; the theory of transport phenomena in solids*; Clarendon Press: Oxford, U.K., 1960.
(33) Chen, G.; Yang, R.; Chen, X. *Journal de Physique IV (Proceedings)* **2005**, *125*, 499−504.
(34) Henry, A. S.; Chen, G. *Journal of Computaional and Theoretical Nanoscience* **2008**, *5*, 1−12.
(35) Majumdar, A.; Bhushan, B. *Journal of Tribology* **1991**, *113*, 1−11.
(36) Esfarjani, K.; Chen, G.; Stokes, H. T. *Phys. Rev. B* **2011**, *84*, 085204.
(37) Dames, C.; Chen, G. *CRC Handbook of Thermoelectrics*; CRC Press, Taylor and Francis: London, U.K., 2006; Chapter 42.

■ NOTE ADDED AFTER ASAP PUBLICATION

This paper was published ASAP on April 23, 2012. Multiple corrections have been made throughout the paper. The revised version was posted on May 9, 2012.